Biochemical and Biophysical Research Communications **290,** 546–551 (2002)
doi:10.1006/bbrc.2001.6222, available online at http://www.idealibrary.com on IDEAL®

# Compact Form of DNA Induced by DNA-Binding Protein HU

Takashi Endo, Naoki Sasaki,[1] Isao Tanaka, and Mitsuo Nakata
*Division of Biological Sciences, Graduate School of Science, Hokkaido University, Kita-ku, Sapporo 060-0810, Japan*

Received December 4, 2001

**Interaction of DNA-binding protein HU from *Bacillus stearothermophilus* (HUBst) with coliphage T2 DNA was investigated by means of a single-duplex DNA chain visualization method using fluorescence microscopy. Fluorescence microscopic images of coliphage T2 DNA molecules were observed as a function of HUBst concentration. The average fluorescence image size of T2 DNA decreased with increase in HUBst concentration to a size comparable to that of a DNA globule induced by polyethylene glycol (PEG) and multivalent cation (MVC). The change to globule-like DNA proceeded gradually and monotonously, in contrast to the coil–globule transition of DNA induced by PEG and MVC. The histogram of the fluorescence image length was essentially a single-modal one throughout the process of conformational change. These results indicate that the process of shrinking of DNA from a random coil to a globule-like one is not of a transitional nature. The interaction of HUBst with DNA and the mechanism of shrinkage are concluded to be different from those of PEG-induced and MVC-induced coil–globule transition of DNA.** 

***Key Words:*** **HU from *Bacillus stearothermophilus*; coliphage T2 DNA; collapse of DNA molecules; fluorescence microscope; histogram; noncooperative phenomenon.**

It is well known that a double-stranded DNA molecule, if extended, must have a macroscopic length. In a biological system, such DNA molecules of macroscopic length are capsulized into micron-sized nuclei in biological cells or nano-sized capsides of bacterial viruses. In the case of eukaryotes, histone, a DNA-binding protein, behaves as a spindle of the double-stranded DNA molecule to construct a nucleosome and then a chromosome, which are compact formed structures of DNA molecules to be capsulized in the nucleus. In the case of prokaryotes, nucleosome-like structures of DNA threads have also been reported (1). HU and HU-like proteins, a group of histone-like DNA-binding proteins, are thought to be involved in the formation of those nucleosome-like structures (2). Structural models of HU-DNA interaction based on the results of X-ray crystallographic and NMR spectroscopic studies have been proposed (3–5). An HU dimer unit grips the DNA molecule by their "arms," and adjacent units are combined together by a hydrophobic interaction, and then the DNA molecule is bent. This model suggests that a certain amount of HU, the conformation of a DNA molecule would be as tightly packed as that in capsides of bacterial viruses. However, there has been no evidence of HU-induced collapse of DNA molecules. It is also known that the conformation of DNA molecules in an aqueous buffer solution becomes compact following the addition of neutral polymers, such as polyethylene glycol (PEG), or multivalent cations (MVC), such as hexamine cobalt, spermine, and spermidine (6–10). The process of the conformational change has been shown to be a cooperative, first-order phase transition that is believed to be identical to the coil–globule transition of synthetic polymers (11, 12).

The aim of this study was to determine whether HU proteins actually make a DNA molecule compact and to determine whether any changes in DNA conformation are transition-like changes like the coil–globule transition induced by PEG and MVC. In this study, HU protein of *Bacillus stearothermophilus* (HUBst), which consists of two identical monomers of 90 amino residues and has a total molecular weight of 19.5 kDa, was used (2, 13). By the interaction with HUBst, DNA molecules will be bent and manifest a change in conformation. Conformational change, or collapse, of DNA molecules was observed using fluorescence microscopic images. Fluorescence microscopy has been used for the study of conformational change of DNA molecules and for analysis of the dynamics of single DNA molecules in solution (8, 9). In those studies, it was shown that long DNA macromolecules with sizes of several tens of micrometers can be visualized by means of fluorescence

[1] To whom correspondence and reprint requests should be addressed.

0006-291X/02 $35.00

microscopy even in a dilute solution. In the present study, using fluorescence microscopy, the size distribution of DNA molecules as a function of HUBst concentration was investigated.

## EXPERIMENTAL PROCEDURES

*Materials.* HU protein was obtained from *Bacillus stearothermophilus* (HUBst) and purified. The methods of protein isolation and purification were identical to those described by Dijk *et al.* (13). In this study, coliphage T2 DNA, which was purchased from Sigma Chemicals Co., Ltd. was used as a DNA sample. The molecular weight of T2 DNA is $1.10 \times 10^8$ Da, corresponding to 160 kb and a contour length of about 50 $\mu$m. Since the critical concentration for a dilute solution of T2-phage DNA has been reported to be 12.9 $\mu$g/ml (10, 14), all of the measurements were performed using 5 $\mu$g/ml of DNA aqueous solution containing 0.2 M NaCl. For this DNA concentration, in order for all of the binding sites to be occupied by HUBst, $5.31 \times 10^{-7}$ M HUBst-dimers is needed stoichiometrically (saturation binding, SB). The value of 9 bp units of the binding site size per HUBst-dimer was used in the calculation. In this paper, HUBst-dimer concentration, $[HUBst]_D$, was used as the DNA-binding protein concentration. The maximum HUBst-dimer concentration used in this experiment was $9.3 \times 10^{-7}$ M. For fluorescence microscopic observation, 4′,6-diamidino-2-phenylindole (DAPI) (5 $\mu$g/ml), a fluorescent dye, and 2-mercaptoethanol (2ME), an antioxidant, were used. To prevent adhesion of DNA molecules to the glassware, which would affect the quantitative measurement, all of the glass vessels and the cover glass plates used for the microscopic observation were coated with silicon resin.

*Methods.* A fluorescence microscopic image of a DNA–HUBst complex was obtained using a Nikon Optiphoto 2 fluorescence microscope with an oil-immersed × 100 objective lens. An exciting beam of 365 nm for DAPI was irradiated, and 400 nm of fluorescent light was observed. The fluorescence image was detected by a Hamamatsu C3077-02 CCD camera and recorded by a video system. The size of the fluorescence DNA image was measured on a video display as a function of $[HUBst]_D$. Since a longer axis length of the fluorescent image of the DNA–HUBst complex was considered to represent chain extensibility (15), the longer axis length $L$ was measured as the DNA size. $L$ was measured for 1000 molecules at each $[HUBst]_D$. Histograms of $L$ at all $[HUBst]_D$ s were drawn. All of the experiments were performed at 293 K.

*Competition of HU–DNA interaction with dye binding to DNA.* From structural investigations, it was revealed that the arms of the HU-dimer when binding to a DNA molecule are buried within minor grooves of the DNA molecule (16), and that HU binds to DNA nonpreferentially with respect to the base sequence. On the other hand, the fluorescent dye DAPI used in this study has been shown to bind to DNA molecule also at the minor groove, though preferentially to AT-rich regions (17, 18). To check the influence of DAPI binding to DNA on the HU-DNA interaction, preliminary fluorescence microscopic experiments were performed for sample solutions prepared in the two ways: (A) 2ME and 5 $\mu$g/ml of DAPI were added to 5 $\mu$g/ml of DNA aqueous solution (with 0.2 M NaCl) and the mixed solution was stirred for 5 min, and then, HUBst aqueous solution (with 0.2 M NaCl) was added to the mixed solution of DNA + DAPI (with 2ME); and (B) HUBst aqueous solution (with 0.2 M NaCl) was added to 5 $\mu$g/ml of DNA aqueous solution (with 0.2 M NaCl) and the mixed solution was stirred for 5 min, and then, 5 $\mu$g/ml of DAPI and 2ME were added to the mixed solution of DNA + HUBst. In both solutions, the final concentration of HUBst-dimer was $9.3 \times 10^{-7}$ M. Fluorescence microscopic images of the DNA–HUBst complex prepared in these two ways were both qualitatively (image size) and quantitatively (size distribution) indistinguishable from each other. Since a DAPI molecule needs a binding site on DNA of the size of 3 bp units, 5 $\mu$g/ml of DAPI solution contains DAPI molecules far excess of a saturation binding to 5$\mu$g/ml of DNA in the sample solution. On the basis of results of preliminary experiments, it was concluded that the DAPI-DNA binding does not affect the essential feature of fluorescence microscopy of DNA-HUBst titration. In this study, the sample solution was prepared by the first method described above.

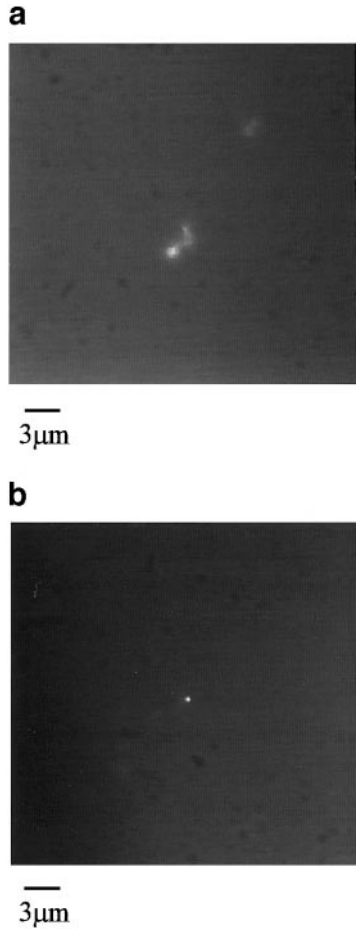


**FIG. 1.** Fluorescent microscopic images of DNA without HU (a) and with $9.3 \times 10^{-7}$ M HU dimer units.

## RESULTS AND DISCUSSION

### *Time Required for Equilibrium Binding*

Figure 1 shows fluorescence microscopic images of DNA with no HUBst (a) and with HUBst-dimer at a concentration of $9.3 \times 10^{-7}$ M (b). A few microns of DNA coil in image (a) becomes an object of about 0.5 $\mu$m in image (b) by adding $9.3 \times 10^{-7}$ M HUBst-dimer. Image (b) was taken at about 60 min after the addition of the HUBst solution to the DNA + DAPI (2ME) mixed solution. In this paper, the longer axis length, $L$, of the fluorescence microscopic image was measured as a parameter representing the size of the DNA–HUBst complex. Fluorescence microscopic images of DNA molecule are known to be affected by the blurring. The

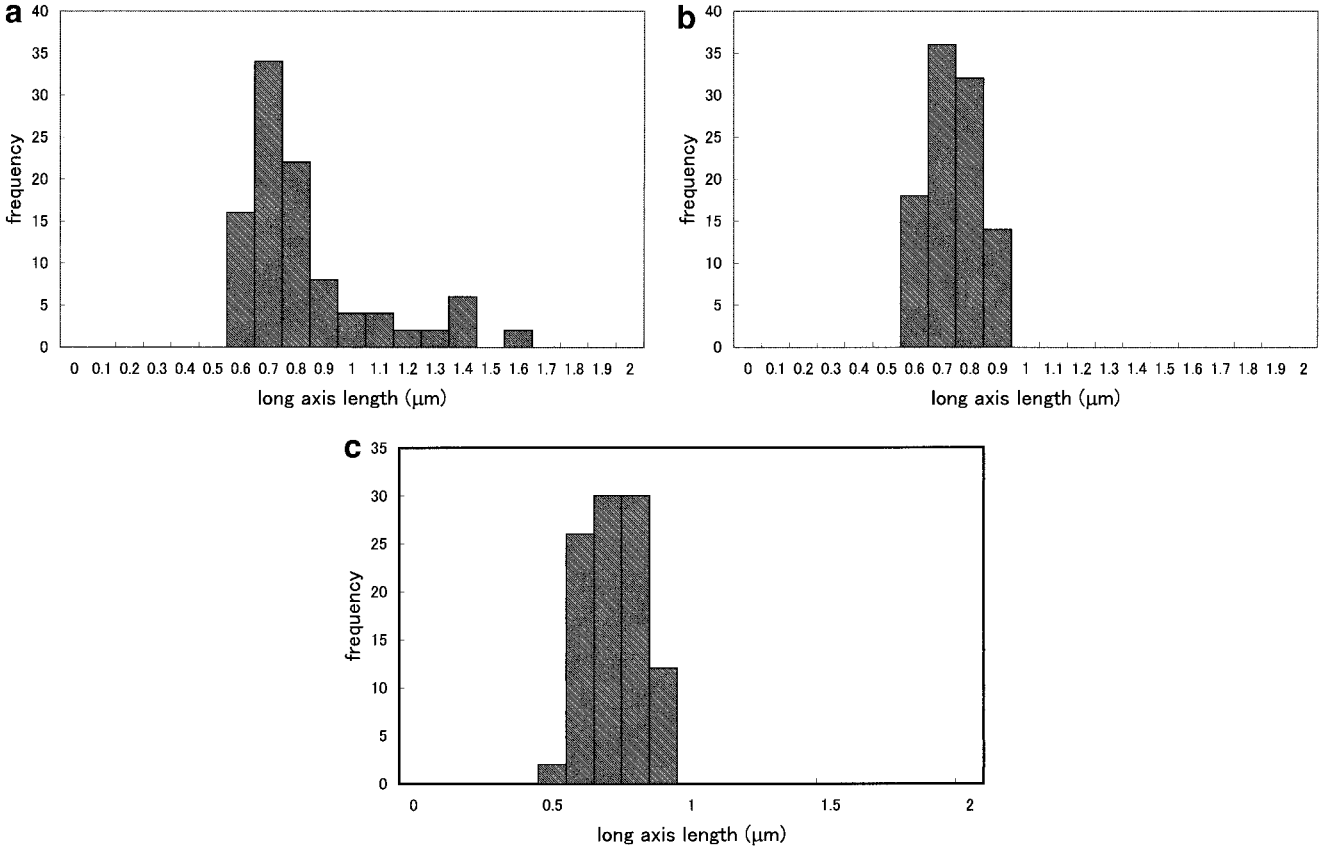


**FIG. 2.** Histograms for the longer axes of fluorescent microscopic images of DNA at 5 min, (b) 20 min, and (c) 50 min after addition of $9.3 \times 10^{-7}$ M $[HUBst]_D$ to an aqueous solution of DNA with 0.2 M NaCl.

actual size of a random coil DNA has been reported to be ~0.3 $\mu$m smaller than that observed by fluorescence microscopy (19).

Figure 2 shows development with time of the histogram of the longer axis length $L$ of fluorescence images of DNA at (a) 5 min, (b) 20 min, and (c) 50 min after the addition of $9.3 \times 10^{-7}$ M HUBst-dimer solution. In Fig. 2a, the histogram has a remarkably longer length-side foot. After 20 min, the foot observed in Fig. 2a had disappeared from the histogram, and the histogram is essentially the same as that in Fig. 2c, indicating that at least 20 min are needed for observation of the equilibrium state of DNA–HU complex. The histograms shown below are constructed for the fluorescence microscopic data taken at more than 60 min after the addition of HUBst.

*Histograms of the Longer Axis of Fluorescence Images of DNA Molecules*

Figure 3 shows histograms of the longer axis length of fluorescence microscopic images of DNA molecules at indicated HUBst-dimer concentrations. A very broad Gaussian-like distribution with an average value of about 3 $\mu$m in the case of no addition of HUBst (Fig. 3a) became a sharp one with an average value of 0.7 $\mu$m following the addition of $9.3 \times 10^{-7}$ M (maximum concentration) of HUBst dimers (Fig. 3c). The single-modal nature of the histogram was not affected by the class width of the histogram. It is clear that HUBst proteins induce a conformational change of DNA from an extended random coil to a compact form of a size comparable to that of the globular state induced by PEG and MVC (10, 19). In the coil–globule transition of DNA observed by PEG and MVC titration, the size distribution of DNA molecules in the transition region was bimodal, indicating the first-order transition nature (20). The single modal nature of the histogram suggests that the conformational change observed here does not have such a transition nature. The binding of HU to DNA has been reported to be noncooperative (21–25). The nontransition nature of the condensing process of DNA revealed here is considered to be related to the noncooperativity of the HU binding to DNA.

In Fig. 4, distribution profiles of DNA–HU complex size are plotted at indicated $[HUBst]_D$s. The distribution profile was calculated on the basis of the histogram. At small $[HUBst]_D$s, height (frequency) of the distribution profile is almost unchanged with the protein concentration but the fluorescent image size at the

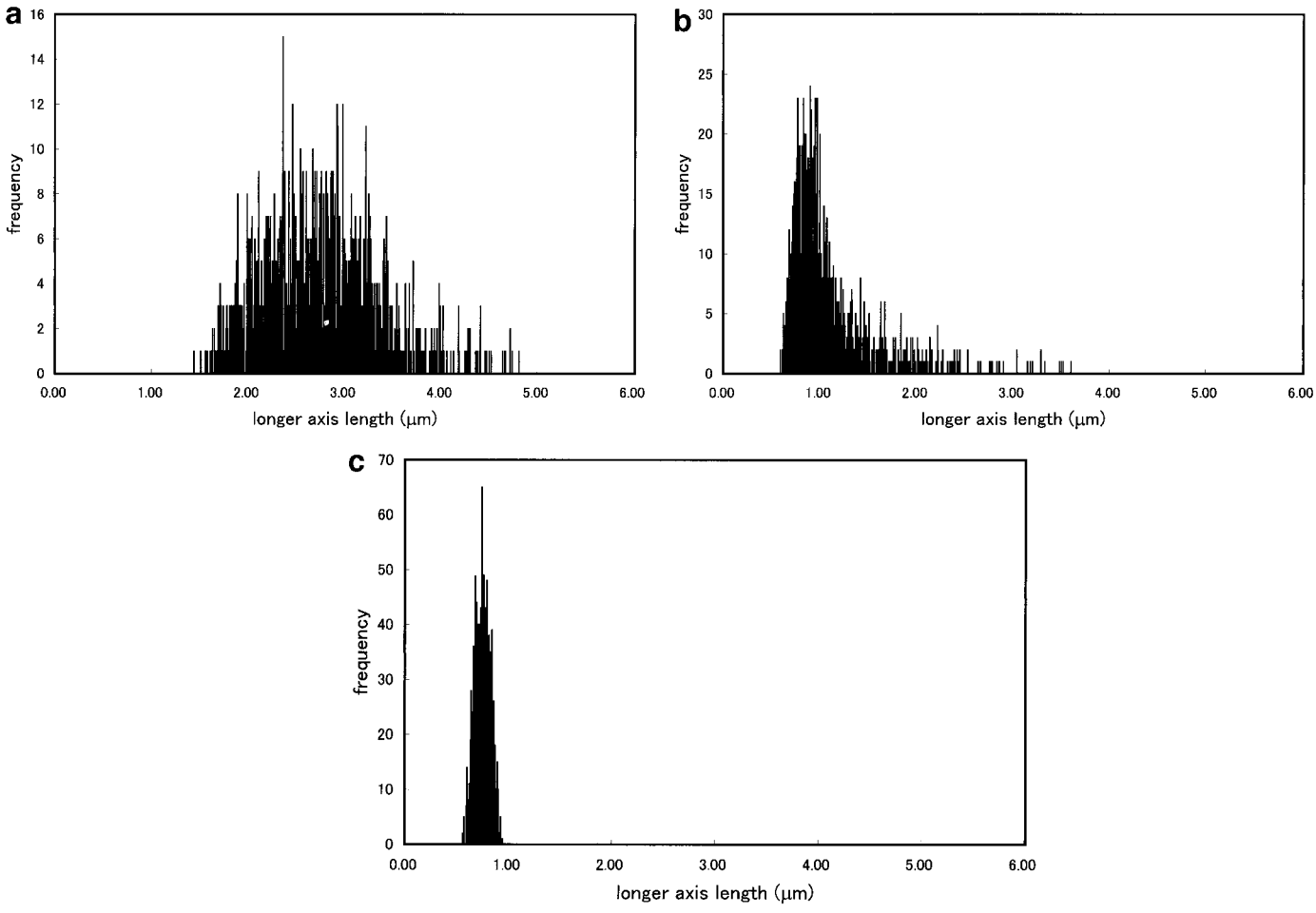


**FIG. 3.** Typical histograms at three different HU concentrations: (a) without HU, (b) $5.6 \times 10^{-7}$ M, and (c) $9.3 \times 10^{-7}$ M $[HUBst]_D$s.

peak of the distribution profile remarkably decreased with elongating the large-size-side foot. At large $[HUBst]_D$s, intensity of the profile increases conspicuously, and the fluorescent image size at the peak of the profile only slightly decreased with decreasing the large-size-side foot. These changes in the distribution profile suggest that the HU binding and DNA condensation process at high protein concentrations is different from those at low HU concentrations.

Figure 5 shows the average size of the DNA–HUBst complex, $< L >$, plotted against HUBst dimer concentration. Vertical lines at data points for $< L >$ are the standard deviation. The horizontal line in the figure indicates the size of globular DNA induced by PEG and MVC (10, 15). Yoshikawa determined the radius of gyration of PEG-induced globular DNA to be ~50 nm on the basis of the Stokes–Einstein law from the translational diffusion constant of PEG-globule (19). It is likely that the radius of gyration of the globule-like DNA–HUBst complex observed here is also similar to this value, though empirical confirmation is needed. The vertical dashed line indicates the $[HUBst]_D$ value at saturation binding (SB). Up to $[HUBst]_D$ of SB, $< L >$ gradually decreased with HU concentration and the standard deviation value (the length of the horizontal bar at each datum point) slightly increased. At HU concentrations larger than SB, $< L >$ leveled off and the standard deviation begun to decrease. The process of conformational change does not have characteristics that indicate coil–globule transition. The results suggest that the conformational change of DNA induced by HUBst is different from those induced by PEG and MVC.

In Fig. 6, three statistical sizes of HU–DNA complex are shown as a function of protein concentration: the mode value, $L_m$, the maximum value, $L_{max}$, and the minimum value, $L_{min}$. The horizontal solid line and the vertical dashed line represent the size of globular DNA induced by PEG and SB concentration of HU, respectively, as in Fig. 5. The curve in the figure represents the average size. The mode value gradually decreases with an increase in $[HUBst]_D$ along with a decrease in the average size. In the region of $[HUBst]_D$s larger than $2 \times 10^{-7}$ M, $[HUBst]_D$ dependence of $L_{min}$ is almost leveled off at the value of 0.5 $\mu$m. In this region, the actual $L_{min}$ is considered to be less than 0.5 $\mu$m. It

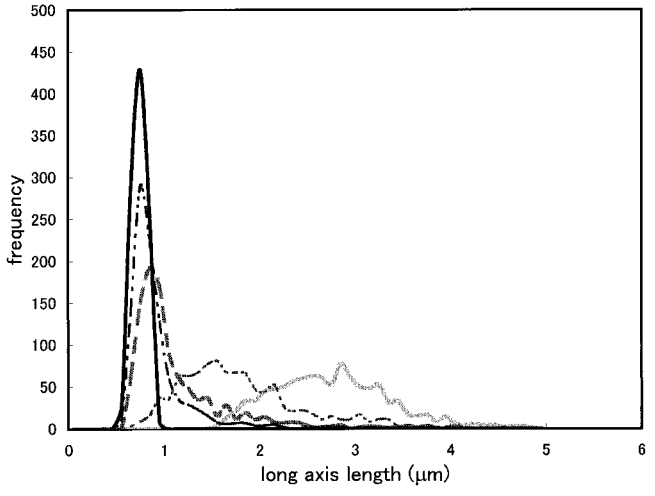


**FIG. 4.** Distribution functions of the longer axis of a fluorescent microscopic image of DNA for 0 $[HUBst]_D$ (—), $1.9 \times 10^{-7}$ M (- - -), $5.6 \times 10^{-7}$ M (– –), $7.5 \times 10^{-7}$ M (– - –), and $9.3 \times 10^{-7}$ M (—) $[HUBst]_D$s.

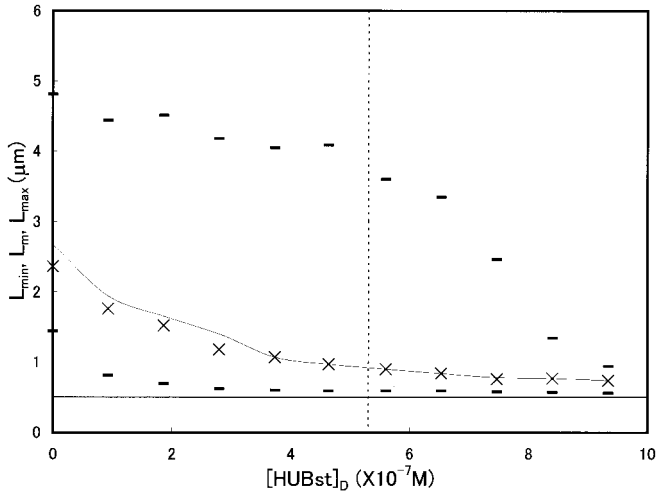


**FIG. 6.** Maximum value, $L_{max}$ (—), minimum value $L_{min}$ (—), and mode value, $L_m$ (×), of a fluorescent microscopic image size of globular DNA plotted against $[HUBst]_D$. The meanings of the horizontal solid line and vertical dashed line are the same as those in Fig. 5. The average value of the fluorescent microscopic image size of DNA is plotted by a solid curve.

is difficult, however, to evaluate a size of the object of less than 0.5 $\mu$m by an optical microscope because of the spatial resolution limit. On the other hand, $L_{max}$ is almost constant up to SB, and for $[HUBst]_D$s larger than SB, it begins to decrease. Figure 7 shows the standard deviation and the skewness of the histogram plotted as a function of $[HUBst]_D$. The standard deviation slightly increases up to SB, and for $[HUBst]_D$s over SB it decreases remarkably. The skewness increases monotonously up to SB and at SB it levels off then decreases to 0. As explained before, the histograms shown in Fig. 3 are those of the equilibrium state. Thus, the skewness is not a transient feature of the HU binding and DNA condensation process.

In Fig. 4, it was concluded that the HU binding and DNA condensation process at high protein concentrations was different from those at low HU concentrations. From the dependence on $[HUBst]_D$ of parameters relating to the size of DNA–HU complex, such as $< L >$, $L_{max}$, $L_{min}$, SD, and the skewness, it is revealed that the suggested change in the quality of the HU binding and DNA condensation process in Fig. 4 occurs in the vicinity of SB. In the absence of HU, DNA molecules are regarded as the random coil just as synthetic polymers in the good solvent. In this state, it is well known that DNA molecules have a broad size

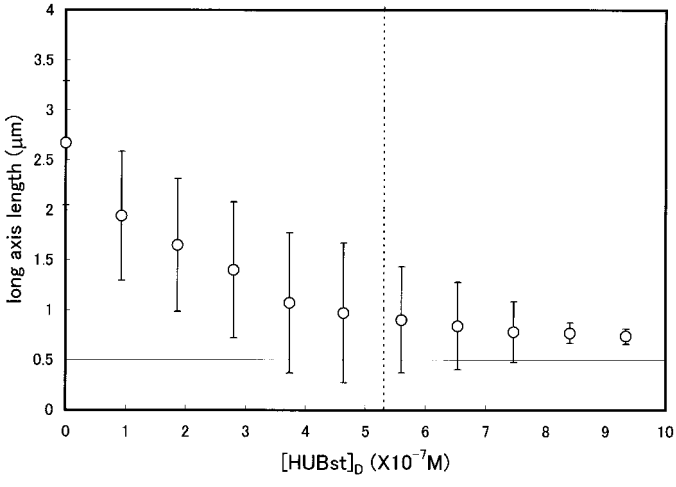


**FIG. 5.** Average of longer axis length plotted against $[HUBst]_D$. The horizontal solid line indicates the fluorescent microscopic image size of globular DNA induced by PEG and MVC. The vertical dashed line indicates the $[HUBst]_D$ value at which all of the DNA sites in the sample solution can be occupied by HU proteins (saturation binding). In the calculation HU-dimer unit was assumed to occupy 9 bp units on a DNA molecule.

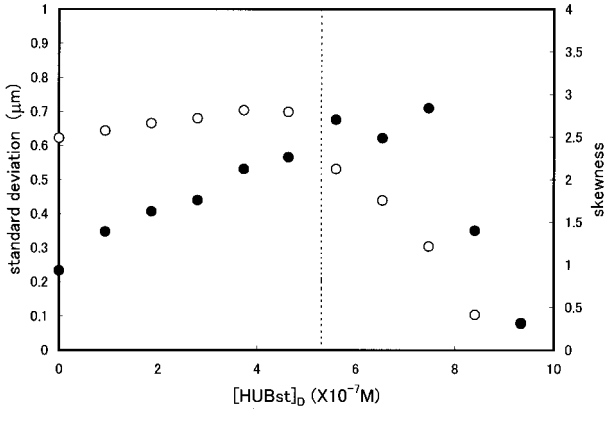


**FIG. 7.** Standard deviation (○) and skewness (●) of the histogram plotted against $[HUBst]_D$. The vertical dashed line indicates the saturation binding value.

distribution (20). In the presence of a small amount of HU, some DNA molecules would be partly bent by the bound HU proteins, while some would remain unchanged. In that case, it is expected that up to SB the average size of DNA molecules would decrease and SD and the skewness would increase with HU concentration. This expectation was confirmed in this study as shown in Figs. 4 and 7. Furthermore, in the solution of HU concentrations larger than SB, both shrunken and still intact DNA molecules must be affected by HU molecules. In Figs. 4 and 5, the decrease in the average size leveled off and the intensity of the distribution peak increased with decreases in larger size-side foot. These findings indicate that DNA that has shrunken would have less susceptibility to further binding of HU proteins, probably because of a steric hindrance.

## CONCLUSIONS

It is clearly observed that T2 DNA molecules become compact due to interaction with HUBst protein molecules to a size comparable to that of PEG- or MVC-induced globular DNA. The average size of fluorescence microscopic images of DNA gradually decreased with increase in HUBst concentration. The histograms of HU-bound DNA at all HU concentrations were essentially single-modal. These results indicate that the change in conformation of DNA induced by HUBst binding is a nontransitional one, unlike those of DNA–PEG or DNA–MVC interactions. Analysis of the histogram revealed that the compacting process at $[HUBst]_D$s larger than SB is different from that at smaller $[HUBst]_D$s.

## ACKNOWLEDGMENT

N.S. is grateful for financial support from the Suhara Memorial Foundation.

## REFERENCES

1. Griffith, J. D. (1976) Visualization of prokaryotic DNA in a regulatory condensed chromatin-like fiber. *Proc. Natl. Acad. Sci. USA* **73,** 563–567.
2. Drlica, K., and Rouvier-Yaniv, J. (1987) Histone-like protein of bacteria. *Microbiol. Rev.* **51**(3), 301–319.
3. Tanaka, I., Appelt, K., Dijk, J., White, S. W., and Wilson, K. S. (1984) 3-A resolution structure of a protein with histone-like properties in prokaryotes. *Nature* **310,** 376–381.
4. Tanaka, H., Yasuzawa, K., Kohno, K., Goshima, N., Kano, Y., Saiki, T., and Imamoto, F. (1995) Role of HU proteins in forming and constraining supercoils of chromosomal DNA in *Escherichia Coli. Mol. Gen. Genet.* **248,** 518–526.
5. Boelens, R., Vis, H., Vorgias, C. E., Wilson, K. S., and Kaptein, R. (1997) Structure and dynamics of the DNA binding protein HU from *Bacillus stearothermophilus* by NMR spectroscopy. *Biopolymers* **40,** 553–559.
6. Laemmli, U. K. (1975) Characterization of DNA condensates induced by poly(ethylene oxide) and polylysine. *Proc. Natl. Acad. Sci. USA* **72**(11), 4288–4292.
7. Gosule, L. C., and Schellman, J. A. (1976) Compact form of DNA induced by spermidine. *Nature* **259,** 333–335.
8. Minagawa, K., Matsuzawa, Y., Yoshikawa, K., Kokhlov, A. R., and Doi, M. (1994) Direct observation of the coil–globule transition in DNA molecules. *Biopolymers* **34,** 555–558.
9. Vasilevskaya, V. V., Khokhlov, A. R., Matsuzawa, Y., and Yoshikawa, K. (1995) Collapse of single DNA molecule in poly(ethylene glycol) solutions. *J. Chem. Phys.* **102,** 6595–6602.
10. Hayakawa, I., Sasaki, N., and Hikichi, K. (1998) The response of DNA macromolecules to an elongational flow field and coil–globule transition of DNA. *Polymer* **39,** 1393–1397.
11. Lifshitz, I. M., Grosberg, A. Yu., and Khokhlov, A. R. (1978) Some problems of the statistical physics of polymer chains with volume interaction. *Rev. Mod. Phys.* **50**(3), 683–713.
12. Sun, Shao-, T., Nishino, I., Swislow, G., and Tanaka, T. (1980) The coil–globule transition: Radius of gyration of polystyrene in cyclohexane. *J. Chem. Phys.* **73**(12), 5971–5975.
13. Dijk, J., White, S., Wilson, K., and Appelt, K. (1983) On the DNA binding protein II from *Bacillus stearothermophilus.* Purification, studies in solution, and crystallization. *J. Biol. Chem.* **258,** 4003–4006.
14. Yanagida, M., Hiraoka, Y., Katsura, I. (1983) Dynamic behaviors of DNA molecules in solution studied by fluorescent microscopy. *Cold Spring Harb. Symp. Quant. Biol.* **47,** 177–187.
15. Mel'nikov, S. M., Sergeyev, V. G., and Yoshikawa, K. (1995) Discrete coil–globule transition of large DNA induced by cationic surfactant. *J. Am. Chem. Soc.* **117,** 2401–2408.
16. Lavoie, B. D., Shaw, G. S., Millner, A., and Chaconas, G. (1996) Anatomy of a flexer–DNA complex inside a higher-order transposition intermediate. *Cell* **85,** 761–771.
17. Kubista, M., Akerman, B., and Norden, B. (1987) Characterization of interaction between DNA and 4′,6-diamidino-2-phenylindole by optical spectroscopy. *Biochemistry* **26,** 4545–4559.
18. Wilson, W. D., Tanious, F. A., Barton, H. J., Jones, R. L., and Strekowski, L. (1990) DNA sequence dependent binding modes of 4′,6-diamidino-2-phenylindole (DAPI). *Biochemistry* **29,** 8452–8461.
19. Yoshikawa, K., and Matsuzawa, Y. (1995) Discrete phase transition of giant DNA dynamics of globule formation from a single molecular chain. *Physica D* **84,** 220–227.
20. Yoshikawa, K., Takahashi, M., Vasilevskaya, V. V., and Khokhlov, A. R. (1996) Large discrete transition in a single DNA molecule appears continuous in ensemble. *Phys. Rev. Lett.* **76**(16), 3029–3031.
21. McGhee, J. D., and von Hippel, P. H. (1974) Theoretical aspects of DNA–protein interactions: Co-operative and non-co-operative binding of ligands to a one-dimensional homogeneous lattice. *J. Mol. Biol.* **86,** 469–489.
22. Kowalczykowski, S. C., Paul, L. S., Lonberg, N., Newport, J. W., McSwiggen, J. A., and von Hippel, P. H. (1986) Cooperative and noncooperative binding of protein ligands to nucleic acid lattices: Experimental approaches to the determination of thermodynamic parameters. *Biochemistry* **25,** 1226–1240.
23. Groch, N., Schindelin, H., Scholtz, A. S., Hahn, U., and Heinemann, U. (1992) Determination of DNA-binding parameters for the *Bacillus subtilis* histone-like HBsu protein through introduction of fluorophores by site-directed mutagenesis of a synthetic gene. *Eur. J. Biochem.* **207,** 677–685.
24. Wojtuszewski, K., Hawkins, M. E., Cole, J. L., and Mukerji, I. (2001) HU binding to DNA: Evidence for multiple complex formation and DNA bending. *Biochemistry* **40,** 2588–2598.
25. Porschke, D. (1984) Dynamics of DNA condensation. *Biochemistry* **23,** 4821–4828.